Articles

Synthesis, Structure, and Electrochemistry of Mononuclear and Face-to-Face Binuclear Orthometalated Complexes of Palladium(II) with N-Monodentate or N(1),N(3)-Bridging 1,3-Di-*p*-tolyltriazenido Ligands. Dependence on Geometrical Arrangement of the Electronic Communication between Two Equivalent Redox Sites

G. García-Herbosa,*,† N. G. Connelly,‡ A. Muñoz,† J. V. Cuevas,† A. G. Orpen,‡ and S. D. Politzer‡

Departamento de Química, Facultad de Ciencias, Universidad de Burgos, 09001 Burgos, Spain, and School of Chemistry, University of Bristol, Bristol, U.K. BS8 1TS

Received January 30, 2001

The synthesis, electrochemistry, and structural characterization of the mononuclear complex [Pd{$C_6H_4N(H)N{=}C(CH_3)C_5H_4N$}(*p*-tolN−N=N*p*-tol)] (**1**) containing the monodentate 1,3-di-*p*-tolyltriazenido ligand is described. Compound **1** is an example of a stable species containing a Pd−N amido bond *cis* to a Pd−C aryl bond. Kinetic parameters for the dynamic intramolecular N(1)−N(3) exchange of the monodentate ligand in complex **1** have been calculated. The *cis* and *trans* isomers of the orthometalated face-to-face complex [{Pd($C_6H_4N{=}NC_6H_5$)(μ-*p*-tolNNN*p*-tol)}$_2$] (**2**) have also been prepared, and the crystal structure of the *trans* isomer is reported. There are noticeable differences in the electrochemical behavior of the mononuclear and binuclear species. From the electrochemical experiments on both isomers of **2** it is possible to recognize different redox sites, to calculate the electronic coupling between them, and to suggest where the reversible electron transfers occur. Each isomers of **2** undergoes two one-electron oxidations and two one-electron reductions. The electronic coupling (ΔE = 0.40 V) at oxidizing potentials is identical for both isomers of complex **2**, suggesting that the oxidations occur on the Pd(μ-triazenido)$_2$Pd framework which is common to both isomers. By contrast, the electronic coupling at reducing potentials is greater for *cis*-**2** (ΔE = 0.33 V) than for *trans*-**2** (ΔE = 0.25 V), suggesting that the reduction processes occur on the orthopalladated fragments, which are arranged differently on the two isomers. Thus, electronic communication between two equivalent redox centers in the same molecule depends not only on the nature of the bridging ligand but also on the geometrical arrangement of the redox centers.

Introduction

The chemistry of the metal−nitrogen amido bond, where M is a late transition metal, continues to attract attention due, among other reasons, to the role of such compounds in stoichiometric or catalytic C−N bond formation.[1,2] Whereas bridging amido complexes of palladium(II) were reported by Okeya in 1982,[3] only a few complexes containing terminal Pd−N amido bonds *trans* to a Pd−C bond have been reported.[4,5] The number of related *cis* complexes, which are the accepted intermediates in the mechanism of C−N bond formation through reductive elimination, has recently been increased by the use of the chelating ancillary ligand dppf {1,1′-bis(diphenylphosphino)ferrocene}.[6] In addition to the role of palladium amido complexes in organic synthesis, we have found that arylamido ligands coordinated to palladium undergo oxidative C−C couplings and formation of tetranuclear complexes with unusual electrochemical properties.[7] The goal of this work was

* Corresponding author. E-mail: gherbosa@ubu.es.
† Universidad de Burgos.
‡ University of Bristol.

(1) Hartwig, J. F. *Angew. Chem., Int. Ed.* **1998**, *37*, 2046.
(2) Müller, T. E.; Beller, M. *Chem. Rev.* **1998**, *98*, 675.
(3) Okeya, S.; Yoshimatsu, H.; Nakamura, Y.; Kawaguchi, S. *Bull. Chem. Soc. Jpn.* **1982**, *55*, 483.
(4) Espinet, P.; García, G.; Herrero, F. J.; Jeannin, Y.; Philoche-Levisalles, M. *Inorg. Chem.* **1989**, *28*, 4207.
(5) Driver, M. S.; Hartwig, J. F. *J. Am. Chem. Soc.* **1995**, *117*, 4708
(6) Driver, M. S.; Hartwig, J. F. *J. Am.Chem. Soc.* **1997**, *119*, 8232.

10.1021/om010075r CCC: $20.00
Publication on Web 06/20/2001

to prepare species containing both Pd−N amido and Pd−C bonds using orthopalladated complexes [Pd{$C_6H_4N(H)N{=}C(CH_3)C_5H_4N$}Cl][8] and [{Pd($C_6H_4N{=}NC_6H_5$)($\mu$-Cl)}$_2$][9] and the 1,3-di-*p*-tolyltriazenido group as the amido ligand. In this paper we report the synthesis, structural characterization, and electrochemical behavior of the mononuclear complex [Pd{$C_6H_4N(H)N{=}C(CH_3)C_5H_4N$}(*p*-tolN−N=N*p*-tol)] (**1**) and the binuclear complexes *cis*- and *trans*-[{Pd($C_6H_4N{=}NC_6H_5$)(μ-*p*-tol-NNN-*p*-tol)}$_2$] (**2**).

Electronic communication between redox sites in binuclear complexes is a subject of great interest not only from the theoretical point of view but also for the potential applications in molecular electronics. Many current articles stress the importance of the bridge connecting the redox sites.[10−14] Electrochemical studies on complexes *cis*-**2** and *trans*-**2** indicate that electronic communication between chemically equivalent redox centers depends not only on the nature of the bridge but also on the geometrical arrangement of the redox-active fragments.

Experimental Section

General Information. All reactions and manipulations were routinely performed under a nitrogen or argon atmosphere using standard Schlenk techniques. Solvents were dried and distilled prior to use. The complexes [Pd{$C_6H_4N(H)N{=}C(CH_3)C_5H_4N$}Cl],[8] [{Pd($C_6H_4N{=}NC_6H_5$)($\mu$-Cl)}$_2$],[9] and 1,3-di-*p*-tolyltriazene[15] were prepared according to published methods. All the other reagents and chemicals were reagent grade and were used as received from commercial suppliers. Elemental analyses (C, H, N) were made on a Perkin-Elmer 2400 instrument. ^{1}H NMR spectra were obtained on a Varian VXR-200S, a Bruker AF-80, or a Bruker AC-300 spectrometer and were referenced to internal TMS and reported on the δ scale. Cyclic voltammetry and differential pulse voltammetry were carried out using EG&G 273 and EG&G VersaStat potentiostats in conjunction with a three-electrode cell using 0.1 M [NBu^n_4][PF_6] solutions in CH_2Cl_2 or tetrahydrofurane, a Pt bead or Pt disk electrode, and the saturated calomel electrode (SCE) as reference. Under the conditions used, $E°'$ for the one-electron oxidation of [Fe(η-C_5Me_5)$_2$], added to the test solutions as an internal calibrant, is −0.08 V.

X-ray Crystal Structure Determinations of 1 and *trans*-2. Crystal data for the structure determinations are collected in Table 1.

Synthesis of [Pd{$C_6H_4N(H)N{=}C(CH_3)C_5H_4N$}(*p*-tolN−N=N*p*-tol)], 1. To a suspension of [Pd{$C_6H_4N(H)N{=}C(CH_3)C_5H_4N$}Cl] (300 mg, 0.85 mmol) in acetone (75 mL) was added 184.7 mg (0.85 mmol) of 1,3-di-*p*-tolyltriazene. After stirring the mixture for 5 min at room temperature a solution (0.53 M) of sodium methoxide (1.6 mL, 0.85 mmol) in methanol was added. The mixture, which was first blue and then reddish-orange 5 min later, was left to stir for 90 min. An orange solid was then collected by filtration and washed with methanol (2 × 10 mL). Anal. Calcd (found) for $PdC_{27}H_{26}N_6$: C, 60.0 (60.4); H, 4.8 (4.9); N, 15.6 (15.8). ^{1}H NMR ($CDCl_3$, 300.13 MHz, 20 °C): δ 13.14 (s, 1H, *NH*), 8.04 (d, 2H, *J*(HH) = 8.4 Hz, *o*-C_6H_4, *p*-tol), 7.68 (m, 1H, H$^{6'}$), 7.66 (d, 2H, *J*(HH) = 8.3 Hz, *o*-C_6H_4, *p*-tol′), 7.46 (td, 1H, *J*(HH) = 8.0, 1.6 Hz, H$^{4'}$), 7.14(d, 2H, *J*(HH) = 8.3 Hz, *m*-C_6H_4, *p*-tol′), 7.08 (d, 2H, *J*(HH) = 8.4 Hz, *m*-C_6H_4, *p*-tol), 6.92 (m, 1H, H$^{5'}$), 6.65 (d, 1H, *J*(HH) = 8.0 Hz, H$^{3'}$), 6.52 (dd, 1H, *J*(HH) ≈ 7.1, 0.9 Hz, H^6), 6.16 (td, 1H, *J*(HH) ≈ 7.2, 1.3 Hz, H^5), 6.02 (dd, 1H, *J*(HH) ≈ 7.7, 1.0 Hz, H^3), 5.94 (td, 1H, *J*(HH) ≈ 7.9, 0.9 Hz, H^4), 2.35 (s, 3H, *Me*, *p*-tol′), 2.32 (s, 3H, *Me*, *p*-tol), 1.93 (s, 3H, *Me*, hydrazone). (Proton numbering of orthometalated ring: H^n. Proton numbering of pyridine ring: H$^{n'}$.)

Crystals of **1**·0.5CH_2Cl_2 were grown by the slow diffusion of Et_2O into a solution of the complex in CH_2Cl_2 under nitrogen at room temperature and protected from light.

Synthesis of *trans*- and *cis*-[{Pd($C_6H_4N{=}NC_6H_5$)(μ-*p*-tolNNN*p*-tol)}$_2$], *trans* and *cis*-2. To a mixture of [{Pd($C_6H_4N{=}NC_6H_5$)(μ-Cl)}$_2$] (800 mg, 1.24 mmol) and 1,3-di-*p*-tolyltriazene (556.5 mg, 2.48 mmol) in CH_2Cl_2 (100 mL) was added a solution (0.53 M) of sodium methoxide (4.7 mL, 2.48 mmol) in methanol. After stirring for 1 h at room temperature the dark brown mixture was filtered through Celite. Addition of *n*-hexane and concentration to induce precipitation afforded a mixture of *cis*-**2** and *trans*-**2** (ca. 1:1 by ^{1}H NMR spectroscopy), which was washed with *n*-hexane (2 × 10 mL) and dried in vacuo. Yield: 1306 mg (95%).

The *cis*-**2** and *trans*-**2** isomers were separated by chromatographing 100 mg of the mixture on a silica gel−*n*-hexane column. Elution of the first band (dark brown) with CH_2Cl_2−*n*-hexane (3:7) gave a solution, which was evaporated to low volume in vacuo to yield 37 mg (yield 74%) of *trans*-**2** as a black solid. Anal. Calcd (found) for $Pd_2C_{52}H_{46}N_{10}$: C, 61.0 (60.4); H, 4.5 (4.5); N, 13.7 (13.6). ^{1}H NMR ($CDCl_3$, 80 MHz): δ 7.54 (m, 14H, aromatic), 6.99 (m, 20H, aromatic), 2.24 (s, 6H, *Me*, *p*-tol), 2.16 (s, 6H, *Me*, *p*-tol′). Cyclic voltammetry of *trans*-**2** (CH_2Cl_2, Pt-disk electrode): $E°'_1 = -1.24$ V, $E°'_2 = -1.03$ V, $E°'_3 = 0.91$ V, $E°'_4 = 1.31$ V versus SCE.

Well-shaped crystals of *trans*-**2**·CH_2Cl_2, suitable for X-ray analysis, were obtained by slow crystallization of the complex from CH_2Cl_2−*n*-hexane solutions under nitrogen at room temperature.

Elution of the second band (dark green) with the same mixture of solvents and similar subsequent treatment of the solution afforded 18 mg (yield 36%) of *cis*-**2** as black microcrystals. Anal. Calcd (found) for $Pd_2C_{52}H_{46}N_{10}$: C, 61.0 (60.5); H, 4.5 (4.6); N, 13.7 (13,6). ^{1}H NMR ($CDCl_3$, 80 MHz): δ 7.57 (m, 11H, aromatic), 6.90 (m, 23H, aromatic), 2.25 (s, 6H, *Me*, *p*-tol), 2.19 (s, 6H, *Me*, *p*-tol′).

Kinetic Studies by Variable-Temperature NMR Spectroscopy. Spectra were obtained using a Varian VXR-200S spectrometer equipped with a variable-temperature unit, calibrated against a standard Varian methyl alcohol sample. The two-site exchange of the triazenido ligand was studied by means of line shape analysis (LSA) of the temperature-dependent resonances corresponding to the methyl protons of the *p*-tolyl groups. The spectra were recorded with good homogeneity at different temperatures and simulated using the program DNMR6 [DNMR6; Quantum Chemical Program Exchange (QCPE633); Indiana University, Bloomington, IN, 1995]. The acceptable value of *k* at each temperature was that for which the simulated and experimental spectra coincided.

Thermodynamic activation parameters were calculated according to Arrhenius and Eyring equations. The $\Delta H^‡$ and $\Delta S^‡$ values were obtained from least-squares treatment of the corresponding rate data. The small magnitude of the chemical shift separation, $\nu_1-\nu_2$, acted as a source of error. Maximum errors of ca. ±1.1 kJ mol^{-1} in $\Delta H^‡$ and E_A and ca. ±3.5 J K^{-1} mol^{-1} in $\Delta S^‡$ were estimated. The effect of the uncertainty in

(7) Espinet, P.; Alonso, M. Y.; García-Herbosa, G.; Ramos, J. M.; Jeannin, Y.; Philoche-Levisalles, M. *Inorg. Chem.* **1992**, *31*, 2502.
(8) García-Herbosa, G.; Muñoz, A.; Miguel, D.; García-Granda, S. *Organometallics* **1994**, *13*, 1775.
(9) Cope, A. C.; Siekman, R. W. *J. Am. Chem. Soc.* **1965**, *87*, 3272.
(10) Astruc, D. *Acc. Chem. Res.* **1997**, *30*, 383.
(11) Fraysse, S.; Coudret, C.; Launay, J. P. *Eu. J. Inorg. Chem.* **2000**, *7*, 1581.
(12) Higuchi, H.; Ishikura, T.; Miyabayashi, K.; Miyake, M.; Yamamoto, K. *Tetrahedron Lett.***1999**, *40*, 9091.
(13) Kheradmandan, S.; Heinze, K.; Schmalle, H. W.; Berke, H. *Angew. Chem., Int. Ed.* **1999**, *38*, 2270.
(14) Ortega, J. V.; Hong, B.; Ghosal, S.; Hemminger, J. C.; Breedlove, B.; Kubiak, C. P. *Inorg. Chem.* **1999**, *38*, 5102.
(15) Furniss, B. S.; Hannaford, A. J.; Smith, P. W. G.; Tatchell, A. R. *Vogel's Textbook of Practical Organic Chemistry*, 5th ed.; Longman Scientific and Technical: Essex, England, 1989.

Table 1. Crystal and Intensity Data for [Pd($C_6H_4NHN{=}C(CH_3)C_5H_4N$)(*p*-tol-NNN-*p*-tol)]·0.5CH_2Cl_2 (1) and for [{Pd($C_6H_4N{=}NC_6H_5$)}$_2${μ-(*p*TolNNN*p*-tol)}$_2$]·CH_2Cl_2 (*trans*-2)

crystal data for **1**		crystal data for *trans*-**2**	
empirical formula	$C_{27.5}H_{26}Cl\ N_6Pd$	empirical formula	$C_{53}H_{48}Cl_2\ N_{10}Pd_2$
color; habit	brown flat cuboids	color; habit	black irregular blocks
cryst size	0.5 × 0.5 × 0.5 mm	cryst size	0.7 × 0.5 × 0.5 mm
cryst syst	monoclinic	cryst syst	triclinic
space group	*C*2/c (No. 15)	space group	$P\bar{1}$
unit cell dimens	a = 22.052(4) Å	unit cell dimens	a = 12.673(5) Å
	b = 22.922(5) Å		b = 13.581(5) Å
	c = 10.263(2) Å		c = 15.893(7) Å
	β = 90.85(1)		α = 94.79(3)°
volume	5187(2) Å^3		$^{\beta}$ = 94.99(4)°
Z	8		γ = 112.45(3)°
fw	582.4	volume	2498(2) Å^3
density(calcd)	1.492 Mg/m^3	Z	2
abs coeff	0.85 mm^{-1}	fw	1108.7
F(000)	2368	density(calcd)	1.474 Mg/m^3
Data Collection		abs coeff	0.874 mm^{-1}
diffractometer used	Siemens R3m/V	F(000)	1124
radiation	Mo Kα (λ = 0.71073 Å)	Data Collection	
temperature	292(2) K	diffractometer used	Siemens R3m/V
2θ range for data collection	3.56−50°	radiation	Mo Kα (λ = 0.71073 Å)
scan type	Wyckoff ω	temperature	292(2) K
scan speed	variable; 1.50−14.65 deg/min in ω	2θ range	3.0−50.0°
standard reflns	3 every 50 reflns	scan type	Wyckoff ω
index ranges	$-26 < h < 26$, $-27 < k < 0$, $0 < l < 12$	scan speed	variable; 1.50−14.65 deg/min in ω
no. of reflns collected	6188	scan range (ω)	2.70°
no. of ind reflns	4575 [R(int) = 0.0484]	standard reflns	3 every 50 reflns
profile fitting	not used	*index ranges*	$0 < h < 15$, $-16 < k < 14$, $-18 < l < 18$
abs corr	semiempirical	no. of reflns collected	9221
Solution and Refinement		no. of ind reflns	8780 [R(int) = 6.88]
refinement method	full-matrix least-squares on F^2	no. of obsd reflns	5840 ($F > 4.0\sigma(F)$)
no. of data/restraints/params	4573/3/323	abs corr	semiempirical
goodness-of-fit on F^2	1.180	min./max. transmn	0.2005/0.2388
final R indices [$I>2\sigma(I)$]	R1 = 0.0859, wR2 = 0.1371	Solution and Refinement	
R indices (all data)	R1 = 0.1817, wR2 = 0.1699	refinement method	full-matrix least-squares
largest diff peak	0.913 e Å^{-3}	quantity minimized	$\sum w(F_o - F_c)^2$
largest diff hole	−0.619 e Å^{-3}	absolute structure	N/A
		extinction corr	N/A
		hydrogen atoms	riding model, fixed isotropic U
		weighting scheme	$w^{-1} = \sigma^2(F) + 0.0004F^2$
		no. of params refined	604
		final R indices (obsd data)	R = 5.21, wR = 5.39
		R indices (all data)	R = 8.60, wR = 5.93
		goodness-of-fit	1.48
		largest and mean Δ/σ	0.001, 0.000
		data-to-param ratio	9.7:1
		largest diff peak	0.76 e Å^{-3}
		largest diff hole	-0.72 e Å^{-3}

the evaluation of the line-width is a minimum at the coalescence temperature because the broadening of the lines due to the exchange is a maximum. For that reason, the $\Delta G^{\ddagger}$ value was calculated from the rate data at the coalescence temperature. The estimated error for $\Delta G^{\ddagger}$ was ±1.9 kJ mol^{-1}.

Results and Discussion

Synthesis. As shown in Scheme 1, treatment of [Pd{$C_6H_4N(H)N{=}C(CH_3)C_5H_4N$}Cl] with 1,3-di-*p*-tolyltriazene and sodium methoxide in acetone affords **1** as a stable orange solid in good yield. Similarly, treatment of [{Pd($C_6H_4N{=}NC_6H_5$)(μ-Cl)}$_2$] with 1,3-di-*p*-tolyltriazene and sodium methoxide in dichloromethane affords **2** as a mixture of *cis* and *trans* isomers, which can be separated by chromatography.

X-ray Structure of 1. Figure 1 shows a thermal ellipsoid plot of complex **1**. Monodentate triazenido complexes are rare, and the Cambridge Structural Database shows, to date, only one such palladium complex, *trans*-[PdCl(PPh_3)$_2$(*p*-tolNNN*p*-tol)].[16a] In that case there is a noticeably short nonbonded contact between the metal and the uncoordinated N(3) atom (2.836 Å), whereas for **1** the Pd−N(3) distance is 3.030 Å (Table 2). Creswell et al. (see below) explained the observed dynamic behavior of *trans*-[PdCl(PPh_3)$_2$-(*p*-tolNNN*p*-tol)] in solution on the basis of this short Pd···N(3) distance.[17] Taking into account the higher steric strain in *trans*-[PdCl(PPh_3)$_2$(*p*-tolNNN*p*-tol)], which contains the bulky PPh_3 ligands, why is the distance Pd···N(3) longer in complex **1**? A possible answer requires a closer look at the structure of **1** as presented in Scheme 2.

The plane of the tolyl group attached to N(3) is at an angle of 5.7° to the plane defined by the three nitrogen atoms, whereas the ring bonded to N(1) is 27.3° out of this plane. This could be a result of the proximity of the N(1) ring substituent to the metal atom in that if it were planar with respect to the N atoms, then an ortho

(16) (a) Bombieri, G.; Immirzi, A.; Toniolo, L. *Inorg. Chem.* **1976**, *15*, 2428. (b) Peregudov, A. S.; Kravtsov, D. N.; Drogunova, G. I.; Starikova, Z. A.; Yanovsky, A. I. *J. Organomet. Chem.* **2000**, *597*, 164.

(17) Creswell, C. J.; Queirós, M. A. M.; Robinson, S. D. *Inorg. Chim. Acta* **1982**, *60*, 157.

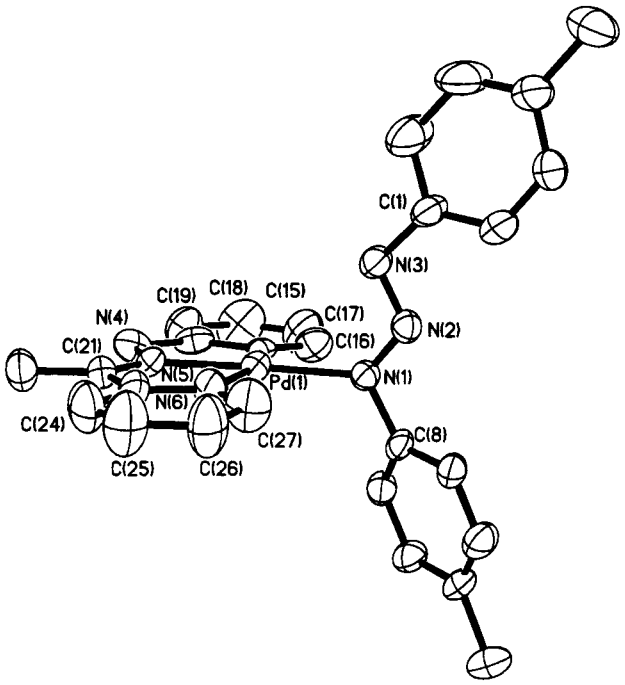

Figure 1. Thermal ellipsoid plot of **1**.

Scheme 1

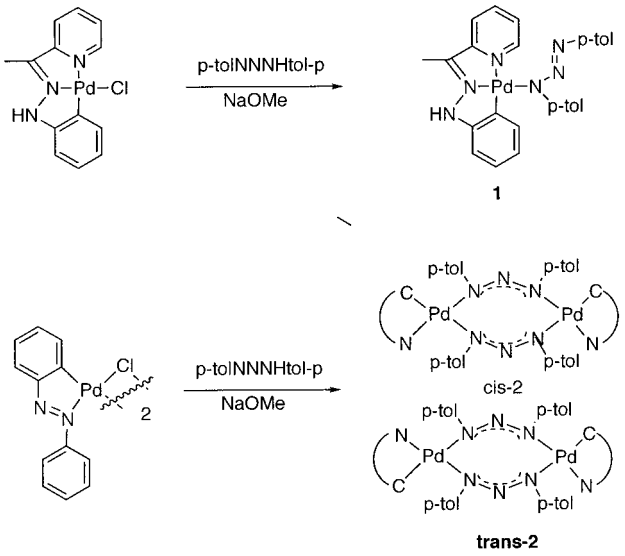

Scheme 2

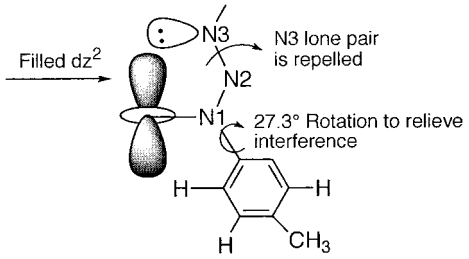

hydrogen would be close to the electron density in the filled metal d_{z^2} orbital. The N(1)−N(2)−N(3) bond angle [116.3(8)°, Table 2] is slightly larger than that of *trans*-[PdCl(PPh$_3$)$_2$(*p*-tolNNN*p*-tol)] (113.0°). Both the bond angles and the nonbonded Pd···N(3) distances indicate larger repulsions in complex **1**. Such repulsions could be explained by describing the bond in terms of the resonance structures 1-i and 1-ii (Scheme 3).

Table 2. Selected Bond Lengths (Å) and Angles (deg) for Complex 1[a]

Pd(1)−C(15)	1.842(13)	Pd(1)−N(5)	1.969(7)
Pd(1)−N(1)	2.034(7)	Pd(1)−N(6)	2.125(8)
N(1)−N(2)	1.294(9)	N(1)−C(8)	1.433(10)
N(2)−N(3)	1.296(9)	N(3)−C(1)	1.421 (11)
N(4)−N(5)	1.344(10)	N(4)−C(20)	1.430(12)
N(5)−C(21)	1.298(11)	N(6)−C(27)	1.338(13)
N(6)−C(23)	1.348(12)	C(1)−C(6)	1.334(13)

C(15)−Pd(1)−N(5)	83.8(5)	C(15)−Pd(1)−N(1)	99.2(4)
N(5)−Pd(1)−N(1)	176.9(3)	C(15)−Pd(1)−N(6)	162.2(4)
N(5)−Pd(1)−N(6)	78.5(4)	N(1)−Pd(1)−N(6)	98.6(3)
N(2)−N(1)−C(8)	113.4(8)	N(2)−N(1)−Pd(1)	125.4(6)
C(8)−N(1)−Pd(1)	118.9(6)	N(1)−N(2)−N(3)	116.3(8)
N(2)−N(3)−C(1)	109.9(8)	N(5)−N(4)−C(20)	109.2(9)
C(21)−N(5)−N(4)	122.6(9)	C(21)−N(5)−Pd(1)	119.9(8)
N(4)−N(5)−Pd(1)	117.4(7)	C(27)−N(6)−C(23)	118.8(10)
C(27)−N(6)−Pd(1)	128.6(8)	C(23)−N(6)−Pd(1)	112.5(8)

[a] Symmetry transformations used to generate equivalent atoms: #1 $-x, y, -z+3/2$.

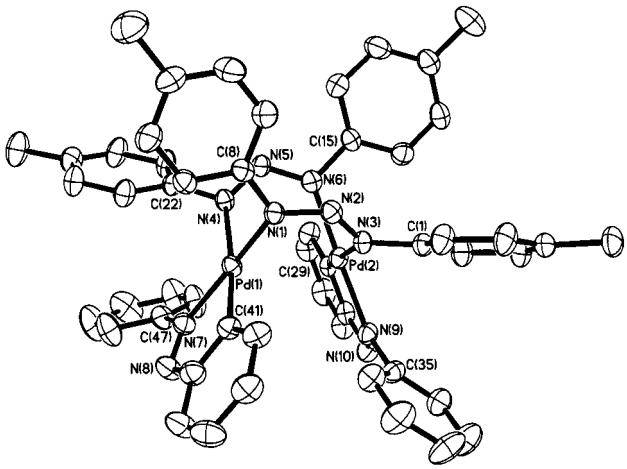

Figure 2. Thermal ellipsoid plot of *trans*-**2**.

Scheme 3

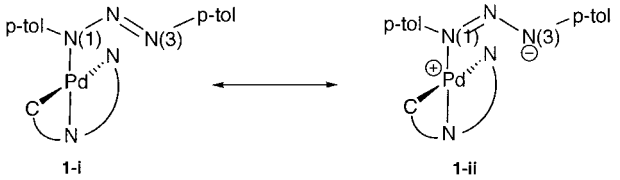

The canonical form 1-ii accumulates negative charge on the uncoordinated N(3) atom, enhancing repulsions with the filled d_{z^2} orbital (see Schemes 2 and 3). The contribution of canonical form 1-ii also accounts for the surprisingly almost identical bond distances N(1)−N(2) [1.294(9) Å] and N(2)−N(3) [1.296(9) Å]. Other monodentate triazenido complexes always show the expected shorter distance for N(2)−N(3) than for N(1)−N(2).[16b] In the complex *trans*-[PdCl(PPh$_3$)$_2$(*p*-tolNNN*p*-tol)] the N(1)−N(2) and N(2)−N(3) distances are 1.336 and 1.286 Å, respectively, indicating a higher contribution of the canonical form 1-i when compared with complex **1**. These results are consistent with the presence or absence of π-acceptor ancillary ligands such as PPh$_3$. Canonical form 1-i must be favored by the presence of π-acceptor ligands. In good agreement with such an assessment, EHMO calculations[18] on the simplified model of complex **1**, [Pd(NHCHCH═NNHCHCH)(HNN-

(18) Mealli, C.; Proserpio, D. M. *J. Chem. Educ.* **1990**, *67*, 399.

Table 3. Selected Bond Lengths (Å) and Angles (deg) for *trans*-2·CH_2Cl_2

Pd(2)−Pd(1)	2.895 (2)	Pd(2)−N(3)	2.145 (5)	Pd(2)−N(6)	2.036 (5)
Pd(2)−N(9)	2.047 (5)	Pd(2)−C(29)	1.972 (6)	Pd(1)−N(1)	2.025 (5)
Pd(1)−N(4)	2.145 (4)	Pd(1)−N(7)	2.044 (6)	Pd(1)−C(41)	1.968 (6)
N(1)−N(2)	1.308 (9)	N(1)−C(8)	1.398 (9)	N(2)−N(3)	1.300 (9)
N(3)−C(1)	1.431 (10)	N(4)−N(5)	1.280 (8)	N(4)−C(22)	1.434 (10)
N(5)−N(6)	1.304 (9)	N(6)−C(15)	1.444 (9)	N(7)−N(8)	1.258 (8)
N(7)−C(47)	1.467 (9)	N(8)−C(46)	1.395 (10)	N(9)−N(10)	1.266 (9)
N(9)−C(35)	1.442 (8)	N(10)−C(34)	1.410 (8)	C(1)−C(2)	1.362 (12)

Pd(1)−Pd(2)−N(3)	76.0(2)	Pd(1)−Pd(2)−N(6)	79.7(2)
N(3)−Pd(2)−N(6)	88.5(2)	Pd(1)−Pd(2)−N(9)	108.2(2)
N(3)−Pd(2)−N(9)	102.2(2)	N(6)−Pd(2)−N(9)	168.0(2)
Pd(1)−Pd(2)−C(29)	112.0(2)	N(3)−Pd(2)−C(29)	171.5(3)
N(6)−Pd(2)−C(29)	90.2(2)	N(9)−Pd(2)−C(29)	78.4(2)
Pd(2)−Pd(1)−N(1)	79.3(2)	Pd(2)−Pd(1)−N(4)	74.7(2)
N(1)−Pd(1)−N(4)	87.7(2)	Pd(2)−Pd(1)−N(7)	110.6(2)
N(1)−Pd(1)−N(7)	167.7(2)	N(4)−Pd(1)−N(7)	101.8(2)
Pd(2)−Pd(1)−C(41)	113.0(2)	N(1)−Pd(1)−C(41)	91.3(2)
N(4)−Pd(1)−C(41)	171.9(3)	N(7)−Pd(1)−C(41)	78.2(3)
Pd(1)−N(1)−N(2)	127.6(4)	Pd(1)−N(1)−C(8)	120.2(5)
N(2)−N(1)−C(8)	112.2(5)	N(1)−N(2)−N(3)	116.1(5)
Pd(2)−N(3)−N(2)	123.5(4)	Pd(2)−N(3)−C(1)	120.6(5)
N(2)−N(3)−C(1)	112.1(5)	Pd(1)−N(4)−N(5)	127.4(4)
Pd(1)−N(4)−C(22)	119.5(4)	N(5)−N(4)−C(22)	111.4(5)

NH)], indicate that N(3) supports a net negative charge of −0.82, whereas in the related triphenylphosphine simplified model complex, *trans*-[PdCl(PH_3)$_2$(HNNNH)], the net charge is −0.74.

X-ray Structure of 2. Figure 2 shows a thermal ellipsoid plot of *trans*-**2**. This compound is dimeric with the palladium atoms in a square-planar geometry. The two palladium centers are bridged by two triazenido ligands arranged *cis* to one another. Each metal atom is also chelated by an orthometalated azobenzene ligand, forming a five-membered ring. These rings are essentially planar, with the metalated benzene ring lying in the same plane as the chelate ring. The other "free" benzene ring is twisted relative to the chelate ring. The azobenzene ligands are arranged *trans* with respect to one another.

In compound *trans*-**2** the Pd···Pd distance (Table 3) is 2.895(2) Å. Although a shorter Pd···Pd distance, 2.747(1) Å, has been reported for two palladium atoms bridged by two triazenido ligands in [{Pd_2(μ-ArNNNAr)$_2$}$_2$(μ-Cl)$_4$],[19] both are formally nonbonding given the 16-electron, square-planar coordination environment of the Pd(II) centers.

As for other binuclear complexes bridged by triazenido ligands, the palladium atoms are not in the plane of the triazenido nitrogen atoms, causing the metal square planes to be mutually twisted. The degree of twist can be measured by the torsion angles N(1)−Pd(1)−Pd(2)−N(3) and N(4)−Pd(1)−Pd(2)−N(6), which are 26.8° and 26.4°, respectively. The dihedral angle between the square planes surrounding the palladium atoms is 42.1°.

Dynamic Behavior. The NMR spectrum shows that complex **1** exhibits dynamic behavior at room temperature, and the coalescence of the signals due to the methyl substituents of the *p*-tolyl groups takes place at 328 ± 1 K. This can be explained by the N(1) and N(3) atoms bonding alternately to the metal. The activation parameters calculated as indicated above are E_A = 54.5 ± 1.1 kJ·mol^{-1}, $\Delta G^{\ddagger}$ = 74.1 ± 1.9 kJ·mol^{-1}, $\Delta H^{\ddagger}$ = 51.7 ± 1.1 kJ·mol^{-1}, and $\Delta S^{\ddagger}$ = −197 ± 3.5 J·mol^{-1}·K^{-1}. The large negative value of $\Delta S^{\ddagger}$ is consistent with an intramolecular associative mechanism through a five-coordinate intermediate, in agreement with those proposed for the complexes *trans*-[PdXL_2(κ^1-RNNNR)] (X = Cl, Br; L = phosphine or arsine, R = *p*-tol or *p*-$MeOC_6H_4$).[16a,17,20] Whereas the activation barriers for *trans*-[PdXL_2(κ^1-RNNNR)] are in the range 33.7 ≤ E_A ≤ 42.3 kJ·mol^{-1}, the larger value for complex **1** could be explained by two effects. First, the Pd···N(3) distance in **1** (3.030 Å) is much longer than 2.836 Å, the distance in *trans*-[PdCl(PPh_3)$_2$(p-tolNNNp-tol)]. Second, the *trans* effect for the halide is stronger than for the N-donors.

Electrochemistry

The mononuclear orthopalladated complexes [Pd{$C_6H_4N(H)N{=}C(CH_3)C_5H_4N$}L][$BF_4$] {L = PPh_3, P(OR)$_3$, 4-$CH_3C_5H_4N$, C_4H_8S (tetrahydrothiophene)} show irreversible oxidations in the range 1.2−1.5 V versus SCE.[21] The binuclear face-to-face orthometalated dipalladium complex containing the same CNN tridentate ligand [(Pd{$C_6H_4N(H)N{=}C(CH_3)C_5H_4N$})$_2$($\mu$-$Ph_2PCH_2PPh_2$)][$BF_4$]$_2$[8] is irreversibly oxidized at 1.20 V.[21] Attempts to isolate and characterize any product through chemical or electrochemical oxidation were unsuccessful probably due to the high potential required to remove electrons from this dicationic complex. To lower the oxidation potential while keeping the face-to-face structure, we attempted to replace the neutral $Ph_2PCH_2PPh_2$ bridge with the anionic di-*p*-tolyl triazenido ligand. As described above, such attempts led to **1**. Cyclic voltammetry of **1** showed an irreversible oxidation wave at 0.3 V, in agreement with previous findings that the formation of Pd−N amido bonds leads to low oxidation potentials.[7] However, despite the accessible potential, all attempts to isolate oxidation products were unsuccessful.

The cyclic voltammogram of *trans*-**2** in dichloromethane (Figure 3a) shows four reversible waves, two oxidations at 0.91 and 1.31 V and two reductions at −1.03 and

(19) Cuevas, J. V.; García-Herbosa, G.; Muñoz, A.; Hickman, S. W.; Orpen, A. G.; Connelly, N. G. *J. Chem. Soc., Dalton Trans.* **1995**, 4127.

(20) Toniolo, L.; Immirzi, A.; Croatto, U.; Bombieri, G. *Inorg. Chim. Acta* **1976**, *19*, 209.

(21) García-Herbosa, G.; Muñoz, A.; Maestri, M. *J. Photochem. Photobiol. A: Chem.* **1994**, *83*, 165.

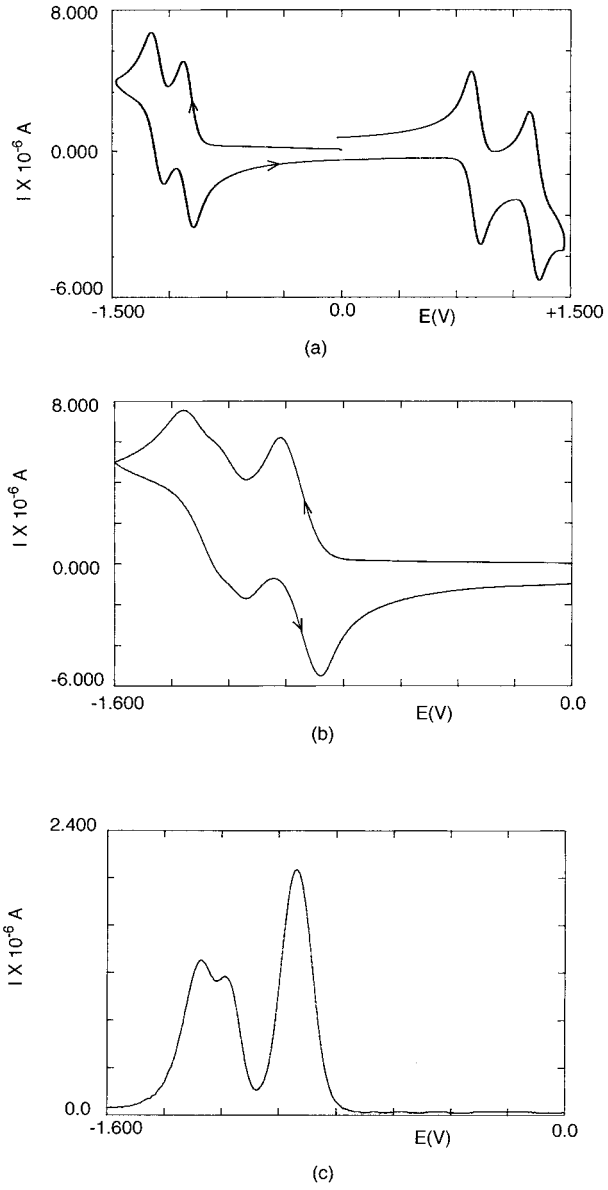

Figure 3. (a) Cyclic voltammogram of *trans*-**2** in dichloromethane, 0.1 M $[NBu^n_4][PF_6]$ at a Pt-disk electrode, scan rate: 200 mV s^{-1}. (b) Cyclic voltammogram of a mixture of *cis*-**2** and *trans*-**2** in tetrahydrofuran; other conditions as in (a). (c) Differential pulse voltammogram of an equimolecular mixture of *cis*-**2** and *trans*-**2** in tetrahydrofuran; other conditions as in (a). Potentials (*E*) are referred to the saturated calomel electrode.

−1.24 V. The four waves have the same limiting current and are therefore associated with the same number of electrons. Although controlled-potential coulometry has not been carried out, the monoelectronic nature of the waves is proposed on the basis of electrochemical studies in structurally related face-to-face compounds.[22]

The isomer *cis*-**2** has a similar CV in CH_2Cl_2 except that the potential for the second reduction wave differs from that of *trans*-**2**; the difference is more clearly seen in the CV (Figure 3b) and DPV (Figure 3c) of a mixture of the two isomers in thf. The first reduction waves of the two isomers are coincident in both solvents. (The oxidation waves occur at potentials too positive to be observed in thf.)

The coordination around palladium in complexes **1** and **2** is almost identical. It consists of one Pd−C(orthometalated) bond, two Pd−N(sp^2) bonds, and one Pd−N(sp^3-amido) bond. The observed shift for the first oxidation potential from 0.31 V in mononuclear complex **1** to 0.91 V in binuclear complexes **2** indicates that the energies of the HOMOs are very different in the two types of complexes. Strictly, only potentials of reversible systems can be directly compared, as the oxidation potential of a chemically irreversible system will also depend on the rate of the reaction following electron transfer. However, the very large difference of 0.7 V cannot be ascribed simply to the fact that one of the two oxidation processes is chemically irreversible.

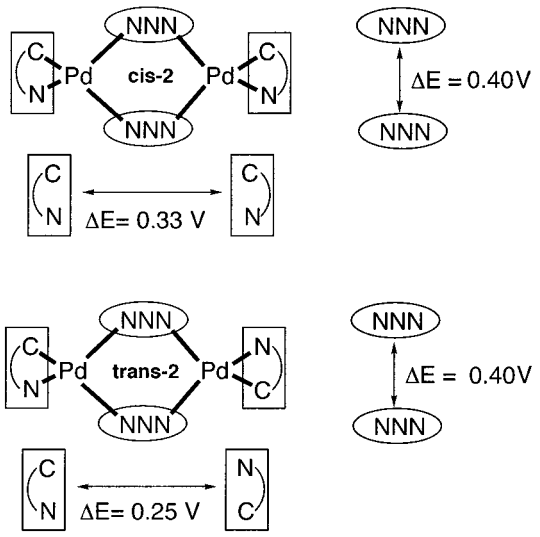

Figure 4. Electronic coupling (communication) between redox sites in *cis*-**2** and *trans*-**2**. (ΔE in volts).

The observed pattern in the CVs of **2** corresponds to binuclear complexes with two equivalent halves, and each half undergoes two reversible electron transfers. Why are the CVs of the *cis* and *trans* isomers coincident apart from the second reduction wave? Although one might expect more differences because the energy levels should be different for both isomers, the energies of the HOMO and LUMO seem to be almost identical for both isomers. The separation between the two oxidation waves (ΔE = 0.40 V) is a measure of the electronic communication (coupling) between the two halves of the mixed valence species $\mathbf{2}^+$, and it is identical in both isomers (see Figure 4).

However, as observed in Figure 3c, the separation between the two reduction waves is different for *cis*-**2** (ΔE = 0.33 V) and *trans*-**2** (ΔE = 0.25 V). This suggests that oxidations occur successively on each half of the Pd(μ-triazenido)$_2$Pd framework (which is identical in both isomers), leading to identical oxidation potentials. On the other hand, the reductions occur successively on each half of the chelate azobenzene orthopalladated (CN)Pd···Pd(CN) framework in the *cis*-**2** case, which is different from the (CN)Pd···Pd(NC) framework in the *trans*-**2** case. The assignment of azobenzene-based reductions when the ligand is orthopalladated has been reported.[23]

In summary, one-half of the redox site of the Pd(μ-triazenido)$_2$Pd framework "feels" the other half to the

(22) Cotton, F. A.; Matusz, M.; Poli, R.; Feng, X. *J. Am. Chem. Soc.* **1988**, *110*, 1144.
(23) Bag, K.; Misra, T. K.; Sinha, C. *Polyhedron* **1998**, *17*, 4109.

same extent in *cis*-**2**$^+$ and *trans*-**2**$^+$, but the first orthopalladated chelate fragment "feels" the second to different extents in *cis*-**2**$^-$ and *trans*-**2**$^-$. This effect is comparable to the magnetic coupling constants between nuclei in NMR spectroscopy, a parameter largely used to distinguish between isomers. The different electronic coupling between the two equivalent redox sites in "(CN)Pd···Pd(CN)" or in "(CN)Pd···Pd(NC)" can only be assigned to the geometrical arrangement of the redox sites, as the bridges are identical in both isomers. Such dependence, of the electronic communication between the two redox sites, not with the bridges but with their geometrical arrangement is, to the best of our knowledge, here reported for the first time.

Conclusions

Orthopalladated complexes react with diaryltriazenide ligands to give stable mononuclear and binuclear compounds containing Pd−N(amido) and Pd−C(aryl) bonds in the *cis* arrangement, which is prone to undergo reductive elimination.[1] In monodentate triazenido complexes the Pd−N(3) distance depends on the donor−acceptor properties of the ancillary ligands coordinated to palladium. This dependence can explain the higher activation energy observed in the fluxional behavior of **1** [corresponding to the N(1) and N(3) atoms bonding alternately to the metal] when compared with that of related complexes if it is accepted that exchange takes place through an associative mechanism.[16a,17,20] Binuclear complexes **2** show very different electrochemical behavior when compared with **1**. They show rich reversible electrochemistry and also an important shift of the oxidation potentials to higher values. The different electronic coupling between the equivalent reduction sites in *trans*-**2** and *cis*-**2** has been ascribed to the geometrical arrangement of the reduction sites as the bridges are identical in both isomers.

Acknowledgment. The authors gratefully acknowledge the Spanish Dirección General de Enseñanza Superior (PB97-0470-C02-02) and the Junta de Castilla y León (BU08/99) for financial support.

Supporting Information Available: Tables of atomic coordinates and equivalent isotropic displacement parameters, bond distances, bond angles, hydrogen coordinates, and anisotropic parameters for the structural analysis of **1** and *trans*-**2** are available free of charge via the Internet at http://pubs.acs.org.

OM010075R